PB83-116996

A Wind Tunnel Study of Dispersion from Sources Downwind of Three-Dimensional Hills

(U.S.) Environmental Sciences Research Lab.
Research Triangle Park, NC

1982

U.S. Department of Commerce
National Technical Information Service
NTIS.

TECHNICAL REPORT DATA
(Please read Instructions on the reverse before completi-

1. REPORT NO.	2.	3.
EPA-600/J-81-470	JOURNAL ARTICLE	PB83-116996

4. TITLE AND SUBTITLE
A WIND TUNNEL STUDY OF DISPERSION FROM SOURCES DOWNWIND OF THREE-DIMENSIONAL HILLS

5. REPORT DATE
1982

6. PERFORMING ORGANIZATION CODE

7. AUTHOR(S)
I.P. Castro and W.H. Snyder

8. PERFORMING ORGANIZATION REPORT NO.

9. PERFORMING ORGANIZATION NAME AND ADDRESS
Environmental Sciences Research Laboratory
Office of Research and Development
U.S. Environmental Protection Agency
Research Triangle Park, NC 27711

10. PROGRAM ELEMENT NO.
CDTA1D/03-1313 (FY-81)

11. CONTRACT/GRANT NO.

12. SPONSORING AGENCY NAME AND ADDRESS
Environmental Sciences Research Laboratory - RTP, NC
Office of Research and Development
U.S. Environmental Protection Agency
Research Triangle Park, NC 27711

13. TYPE OF REPORT AND PERIOD COVERED

14. SPONSORING AGENCY CODE
EPA/600/09

15. SUPPLEMENTARY NOTES
REF: Atmospheric Environment, 16(8):1869-1887, 1982

16. ABSTRACT

The nature of the separated flow fields downwind of moderately steep hills of varying crosswind aspect ratios has been examined using models placed in a simulated adiabatic atmospheric boundary layer in a meteorological wind tunnel. The hills ranged from an axisymmetric cone to a two-dimensional ridge. Concentration patterns resulting from sources placed at numerous heights and distances downwind of these hills were examined. Effective stack heights and amplification factors (i.e., ratios of maximum ground-level concentrations in the presence of the hills to those in the absence of the hills) were used to characterize the effects of the hills on plume transport and diffusion. Amplification factors were generally found to increase as the aspect ratio increased and as the source height approached the reattachment streamline (such that the plume was advected toward the ground). The largest amplification factor (A = 11) was observed when the source was placed halfway from the hill center to the reattachment point at a height of 1 1/4 hill heights downwind of the two-dimensional ridge.

17. KEY WORDS AND DOCUMENT ANALYSIS

a. DESCRIPTORS	b. IDENTIFIERS/OPEN ENDED TERMS	c. COSATI Field/Group

REPRODUCED BY
NATIONAL TECHNICAL
INFORMATION SERVICE
U.S. DEPARTMENT OF COMMERCE
SPRINGFIELD, VA 22161

18. DISTRIBUTION STATEMENT	19. SECURITY CLASS *(This Report)*	21. NO. OF PAGES
RELEASE TO PUBLIC	UNCLASSIFIED	20
	20. SECURITY CLASS *(This page)* UNCLASSIFIED	22. PRICE

EPA Form 2220-1 (9-73)

Atmospheric Environment Vol. 16, No. 8, pp. 1869–1887, 1982
Printed in Great Britain.

EPA-600/J-81-470
JOURNAL ARTICLE

A WIND TUNNEL STUDY OF DISPERSION FROM SOURCES DOWNWIND OF THREE-DIMENSIONAL HILLS

I. P. CASTRO
Department of Mechanical Engineering, University of Surrey, Guildford, Surrey GU2 5XH, U.K.

and

W. H. SNYDER*
Meteorology and Assessment Division, U.S. Environmental Protection Agency, Research Triangle Park, NC 27711, U.S.A.

(*First received* 1 *May* 1981 *and in final form* 28 *September* 1981)

Abstract—The nature of the separated flow fields downwind of moderately steep hills of varying crosswind aspect ratios (spanwise breadth/height) has been examined using models placed in a simulated adiabatic atmospheric boundary layer in a meteorological wind tunnel. The hills ranged from an axisymmetric cone to a two-dimensional ridge. Concentration patterns resulting from sources placed at numerous heights and distances downwind of these hills were examined. Effective stack heights and amplification factors (i.e. ratios of maximum ground-level concentrations in the presence of the hills to those in the absence of the hills) were used to characterize the effects of the hills on plume transport and diffusion. Amplification factors were generally found to increase as the aspect ratio increased and as the source height approached the re-attachment streamline (such that the plume was advected toward the ground). The largest amplification factor ($A = 11$) was observed when the source was placed halfway from the hill center to the re-attachment point at a height of 1 1/4 hill heights downwind of the two-dimensional ridge.

1. INTRODUCTION

Despite the large number of isolated field measurements of concentrations due to one or more effluent sources in complex terrain, and a more limited number of wind tunnel investigations, there is still only partial understanding of the physics of the dispersion processes involved. Most of the reported measurements have been made during laboratory studies of particular sites and only relatively recently have specific attempts been made to isolate the effects of the important parameters. Some of the common effects of complex terrain on the atmospheric boundary layer and the consequent changes in the dispersion processes have been qualitatively evident for some time (e.g. Halitsky, 1968; Scorer, 1968; Strom, 1976), but quantitative information generally does not exist.

These remarks are particularly true in the case of sources downwind of large surface features such as hills, escarpments or large buildings. While it is well known that such features can significantly affect mean plume paths and plume growth rates, the magnitude of the consequent changes in ground-level concentration (GLC) is often not known. The sensitivity of the GLC to changes in the geometry of the surface feature and/or variations in the characteristics of the upstream flow is also unknown. Recent work at the Fluid Modeling Facility of the U.S. Environmental Protection Agency has included investigations of diffusion from sources placed up- and downwind of two-dimensional low but steep ridges (Huber *et al.*, 1976; Arya *et al.*, 1981), two-dimensional hills of moderate slope (Khurshudyan *et al.*, 1981), and steep three-dimensional hills (Snyder and Britter, 1979b).

The last of these investigations was concerned only with upwind sources (3.6h from the hill centerline, where h is the hill height) and with the effect of hill spanwise aspect ratio (breadth/height). Each hill had a triangular side elevation with a slope of 1 in 2 and was therefore sufficiently steep and sharp-edged to ensure separation at or near the peak. Measurements of the flow field and the GLC's on the hill surfaces were made, particular attention being paid to the value of the maximum GLC, C_{gmx}, compared with its value in the absence of the hill, C°_{gmx}, for a source at the same height. At least for source heights H_s less than h, it was found that the amplification A defined by C_{gmx}/C°_{gmx} did not exceed about 4 and was always greater for small-aspect-ratio hills (e.g. a cone) than for wider hills. For small-aspect-ratio hills, as the experiments and theory of Hunt and Snyder (1980) suggest, the mean streamlines pass closer to the hill surface than they do for wider hills, tending to increase GLC's on the hill surface. By contrast, since hills with the larger spanwise widths must, in general, induce stronger plume downwash and have more extensive highly turbulent wakes, it seems likely that A could be considerably greater than 4 for sources placed downwind of the hills. Indeed, the results of Khurshudyan *et al.* (1981) and

* On assignment from the National Oceanic and Atmospheric Administration, U.S. Department of Commerce.

Arya *et al.* (1981) show that A can be at least 10 for sources downwind of two-dimensional hills, even when the hills are not sufficiently steep to promote separation.

The present work, part of EPA's ongoing program, is a study of the effects of changes in hill aspect ratio on the GLC's arising from sources placed at various heights within, above or beyond the near-wake region downwind of the hill. We used the same hills as used by Snyder and Britter (1979b). The near wake contained, in each case, a highly turbulent reversed-flow region which we will loosely call the "cavity"*, recognizing that such a feature exists only in the mean and that, in general, the streamlines separating from the hill surface are not those that re-attach farther downstream (Hunt *et al.*, 1978). By making detailed measurements of GLC's, we hoped to determine, by implication, the effect of different aspect ratios on the dominant physical phenomena in their wakes (e.g. at what aspect ratio does axial vorticity become important, if ever?) and, explicitly, which source locations lead to the greatest amplifications.

Assuming the dynamics of the wake flow to be basically similar for all hills (which is certainly not true under non-neutral conditions, but is more likely to be the case for neutral flow), then the diffusion processes occurring not too far downstream of the recirculating region should scale on some length appropriate to the "hill plus its cavity zone". If, for example, the cavity zone extended downstream a distance x_R from the center of the hill and the source was located at a fixed height at cx_R downstream (where $c > 1$ but not too large), then we might expect downwind concentration fields to collapse for all hill aspect ratios. However, if the wake dynamics (influence of axial vorticity, decay rate of velocity and turbulence perturbations, etc.) depended strongly on hill aspect ratio, then such a collapse would be inherently less likely. With these ideas in mind, the study was undertaken in two stages. First, measurements of the velocity and turbulence fields in the near wake of each hill were made to determine the general shape and extent of the cavity zone and, in particular, to find the positions of reattachment x_R, at least on the hill centerlines. Secondly, sources were placed at up to five heights, $0.25 < H_s/h < 2.0$, and at fixed downstream locations given by cx_R with $c = 0.5$, 1.0 and 1.5 for each hill, and the resulting centerline GLC variations were measured from as far upstream of the source as necessary, to as far downstream as the wind tunnel working section would allow. From a practical point of view, the surface concentration values were likely to be of most direct use. Vertical and elevated spanwise distributions are necessary (since they lead to determination of plume growth rates) for a full physical understanding of the dispersion processes. However, only a limited number of vertical and elevated spanwise distributions were measured; time did not allow a complete investigation of the full concentration field for each case.

* A referee pointed out the inappropriateness of the term "cavity". We agree entirely, but crave the indulgence of the reader in our continued use of the word for the sake of brevity; it should be understood to mean simply "the turbulent, recirculating region immediately behind the hill".

2. EXPERIMENTAL ARRANGEMENTS

2.1. *Apparatus and instrumentation*

All the experimental work was conducted in the EPA Fluid Modeling Facility's low-speed, open-return Meteorological Wind Tunnel, which has a working section 3.7 m wide, 2.1 m high and 18.3 m long and is described in detail by Snyder (1979). A neutrally stable atmospheric boundary layer was simulated using a 153 mm high fence placed just downstream of the contraction exit and followed by gravel roughness, with dimensions up to about 10 mm, covering the whole of the test-section floor. The characteristics of the resulting boundary layer, which was about 800 mm thick at the location where the hills were mounted (8.5 m downstream of the fence), are presented in Section 2.2.

The hills were similar to those used in the earlier study (Snyder and Britter, 1979b) except that they were covered with the same gravel roughness as used for the surrounding surface. They ranged from a simple cone, of base diameter equal to $4h$, to a two-dimensional ridge with the same cross-sectional shape. Intermediate aspect ratios (see Fig. 1) were obtained by inserting straight-sided triangular sections between the two halves of the basic cone. h was nominally 245 mm, so that h/δ, where δ is the boundary layer height, was about 0.30.

Hill	C2	C4	C6	CX
L_1, cm	0	45	90	∞
L, cm	46	91	136	∞
L/h	2.0	3.9	5.8	∞

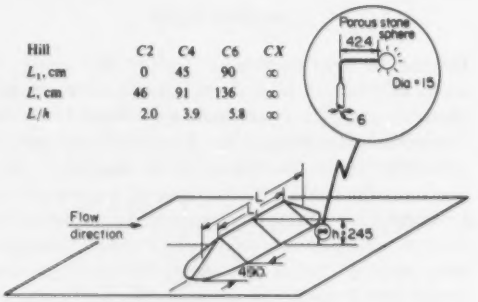

Fig. 1. Details of hills and sources. Dimensions in mm.

All velocity and turbulence measurements behind the hills were made with a pulsed-wire anemometer (Bradbury and Castro, 1971) operated on-line to the facility's PDP 11/40 minicomputer. Probes were calibrated in the free-stream against a standard pitot-static tube, using the relation $U = A/T + B/T^2$, where U is the velocity, T is the time of flight (measured digitally by the anemometer), and A and B are constants. A least-squares fitting procedure was used, and calibration data rarely differed from the final fit by more than one or two per cent. For the actual measurements, the maximum sampling rate used was 60 Hz and the sampling time was typically 90–120 s—long enough to average the low frequency motions reasonably well and to ensure sufficient individual samples to make statistical errors arising from a finite sampling size insignificant, at least for the mean speed U and the variance $\overline{u^2}$. Higher order moments, $\overline{u^3}$ and $\overline{u^4}$, were measured also but invariably showed more scatter; accurate measurements of these would have required considerably longer sampling times.

Apart from the laser–doppler anemometer, the pulsed-wire is the only instrument capable of making reasonably accurate measurements in highly turbulent, reversing flow regions. We believe that these are the first such measurements of flow in the near wake behind model hills sufficiently steep to promote separation, although measurements behind sharp-edged bodies (buildings) are becoming more frequent (e.g. Castro and Robins, 1977; Britter and Hunt, 1979; Davies *et al.*, 1980).

Standard instrumentation (hot-wire anemometry, etc.) was used to calibrate the simulated boundary layer and it too was operated on-line to the PDP 11/40. For the concentration measurements, ethylene (C_2H_4) was used as a tracer gas. It has a density only slightly different from that of air so that it is essentially neutrally buoyant. Since, in many cases, the effluent source would be within the cavity region behind the hill, a porous sphere was used to introduce the tracer into the flow, an arrangement similar to that used in an earlier study (Khurshudyan *et al.*, 1981). The tracer was emitted from a porous stone (or, later, sintered bronze) sphere of diameter 15 mm, at the end of a stack with a 90° bend (Fig. 1). Although large in comparison with a more usual stack diameter, the sphere was small compared to the scale of the flow and the surface emission velocity was typically only about 4% of the free-stream velocity. The volume flow rate Q was usually about 7000 cu^2 min^{-1} and was continuously monitored using a calibrated Meriam laminar-flow element and a micromanometer. Concentration profiles, including surface profiles, were obtained by collecting up to four simultaneous samples through a variety of rakes of 1.6 mm OD tubes which, like all other probes used in the study, could be traversed continuously in all three directions (Snyder, 1979). Samples were drawn through Beckman hydrocarbon analyzers whose outputs were digitized at a rate of 1 Hz and averaged on-line by the PDP 11/40. Since the wind tunnel is an open-return type, there was a gradual build-up of the background level of ethylene in the laboratory. A fifth sample simultaneously collected from the free stream well upwind of the hill was similarly analyzed and used to correct the other four measurements. The software also normalized the corrected concentrations by

$$C = C' U_r h^2 / Q,$$

where C' is the corrected value (parts ethylene per part air by volume), U_r is the free-stream velocity, h is the hill height (taken as 245 mm throughout) and Q is the source volume flow rate. Two-minute averages were usually found to be sufficient.

The analyzers were checked for linearity within, and consistency between, ranges down to very low concentrations using an exponential dilution technique described by Williams and Winefordner (1966). This method provides absolute accuracy without having to rely on standard bottled ethylene/air mixtures. All five analyzers gave excellent linearity over the four decades used during the wind tunnel measurements, apart from slight deviations at the lowest range; possible zero errors of up to 1/2 ppm at most could always account for those. Full-scale and zero levels were set prior to each traverse, measured again at the end and used by the software to make appropriate corrections for drift when necessary.

Apart from a few Reynolds-number tests, all measurements were made at a nominal free-stream velocity of 4 m s^{-1}. Since the tunnel was equipped with an adjustable ceiling, it was possible to conduct all tests under the condition of zero-longitudinal-pressure gradient in the free stream, even with the hills in place.

2.2. *The undisturbed boundary layer*

Complete details of the development and calibration of the simulated boundary layer used in the present study are given by Snyder and Britter (1979a) and Courtney and Britter (1979); only salient results are repeated here. Figures 2 and 3 show mean velocity and Reynolds-stress profiles measured at about 8 m downstream from the fence (hills were placed 8.5 m downstream). The surface-friction velocity implied by the crossed-wire shear-stress measurements ($u_*/U_r = 0.048$) leads to the mean velocity log–law plot shown in Fig. 2(b), corresponding to a surface roughness length of about 0.13 mm and a zero-plane-displacement height of about 2 mm. There was some variability in the latter value, dependent upon which particular data set was used (a number of different studies at various times were made of this particular flow), but in general the scatter between different data sets shown in Figs 2 and 3 was considered acceptable, particularly in view of the various probes and analytical methods used to obtain the data.

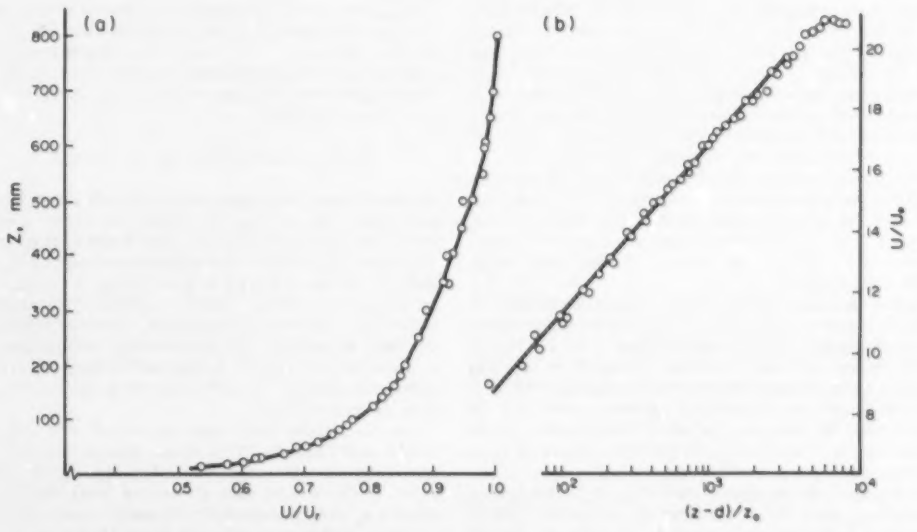

Fig. 2. Mean velocity profiles over gravel roughness 8 mm downwind of fence: (a) linear plot, (b) semi-logarithmic plot.

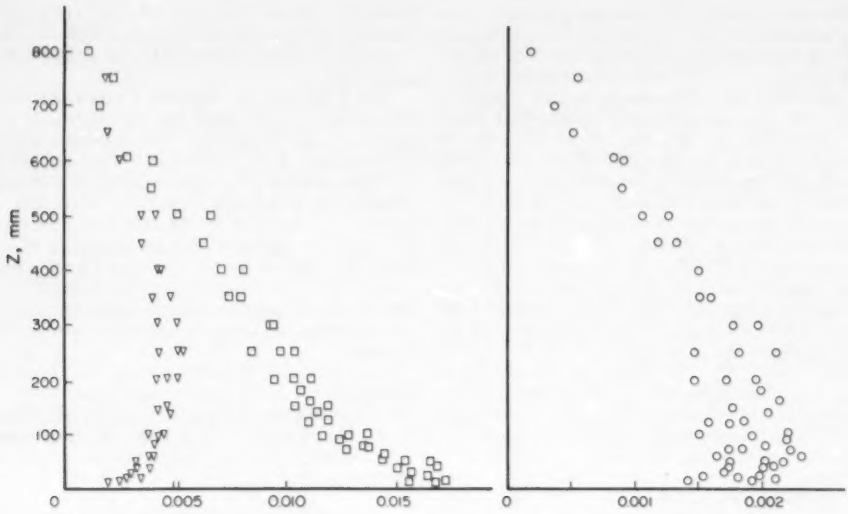

Fig. 3. Reynolds stress profiles over gravel roughness 8 m downwind of fence: (a) □, $\overline{u^2}/U_r^2$; Δ, $\overline{w^2}/U_r^2$; (b) ○, $\overline{uw}/U_r^2$.

Taking the atmospheric boundary layer to be 600 m thick, the equivalent full-scale roughness length was about 10 cm; the simulated flow is clearly representative of a "moderately rough rural type" atmospheric boundary layer (Counihan, 1975). As is usual for flows generated in this way, the outer layer wake component (Coles, 1956) is much weaker than it is in naturally grown boundary layers. Indeed, as Fig. 2(b) shows, it is practically nonexistent and even weaker than it is in flows generated using the Counihan (1969) "fence + vorticity generator + roughness" technique (cf. Robins, 1979). However, measurements at other axial positions showed that the flow was in approximate equilibrium at the hill location. Since h/δ was only 0.3 and, in any case, the outer region of the atmospheric boundary layer is probably quite unlike that of a rough-wall layer grown naturally in the laboratory, this outer layer peculiarity was of no consequence for the present purposes. Spanwise measurements demonstrated that the flow was adequately two-dimensional over at least the central two meters of tunnel width, and tests at various free-stream speeds showed that only for $U_r \leqslant 2\,\mathrm{m\,s^{-1}}$ did Reynolds-number effects become significant.

As "baseline" data on surface concentrations from sources of various heights, we present a representative set measured earlier in the same boundary layer by Khurshudyan *et al.* (1981). Figure 4 shows the axial variation of surface concentration for sources at heights within the range $0.036 \leqslant H_s/\delta \leqslant 0.44$.

Measurements of plume growth rates indicated that the diffusive characteristics of the boundary layer were similar to those of Pasquill–Gifford stability class C to D (Turner, 1970), typical of boundary layers generated in this way (Robins, 1978). Surface concentration profiles for an effective stack height of 45 m (i.e. assuming a geometric scale factor of 770:1) predicted using the Pasquill–Gifford scheme are also shown on Fig. 4, confirming the diffusive characteristics as between stability classes C and D.

In Figure 5, the maximum value $C^\circ_{\phi mx}$ is plotted against distance x_{mx} from the source. None of the standard theories for plume dispersion are, in principle, adequate for elevated sources, since there is no satisfactory way of predicting vertical spread. However, gradient-transfer theory may be applicable in the vicinity of the maximum surface concentration, since there the vertical scale of the concentration field may exceed that of the turbulence (certainly not the case nearer the source). On that basis Moore (1975) used a Gaussian model, allowing for different vertical dispersion above and below the plume centerline and reflection at the ground, to estimate the ground-level concentration. Robins and Fackrell (1979) have shown that this implies $C^\circ_{\phi mx} \propto x_{mx}^{-3/2}$ for sources not too near the ground (see also Pasquill, 1974). The data of Fig. 5 are consistent with this result.

Similarity among the various profiles shown in Fig. 4 is demonstrated in Fig. 6, in which normalized concentrations $C^\circ_\phi/C^\circ_{\phi mx}$ are plotted as functions of distance normalized by distance to the point of maximum concentration x/x_{mx}. Using standard power-law assumptions, it is possible to obtain an analytic solution to the diffusion equation which provides the following universal expression for $C^\circ_\phi/C^\circ_{\phi mx}$ and is independent of source height:

$$C^\circ_\phi/C^\circ_{\phi mx} = \exp\{3/2(1-x_{mx}/x)\}/(x/x_{mx})^{3/2}.$$

The experimental data agree reasonably well with this result, particularly for $x > x_{mx}$. To obtain the above solution, vertical and lateral plume widths were assumed to grow like $x^{1/2}$ and x, respectively. A less restrictive assumption, $\sigma_z \propto x^p$ and $\sigma_y \propto x^q$, can be shown to give $C^\circ_\phi/C^\circ_{\phi mx} \propto (x/x_{mx})^{-(p+q)}$ for $x/x_{mx} >> 1$. Since, at least for ground-level sources, $p \simeq 0.8$ and $q \simeq 0.67$ in the present case, it is not surprising that the data follow the 3/2-law relatively well despite the inadequacies in the theory. Robins and Fackrell (1979) give a useful discussion of the difficulties of predicting diffusion from elevated sources.

Data for ground-level sources agree well with results of Robins and Fackrell (1979), whose measurements encompassed a much wider range of boundary-layer characteristics. Figure 7 shows their data, normalized using surface parameters u_* and z_0, compared with similar measurements of Arya *et al.* (1981) and Snyder and Britter (1979b) made in the present boundary layer. These results reinforced our confidence that the simulated boundary layer was quite adequate.

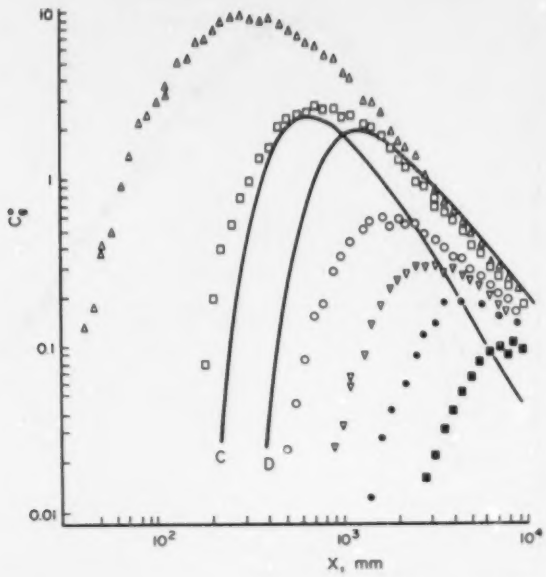

Fig. 4. Surface concentration profiles downwind of stacks of various heights in flat terrain: $h/\delta = 0.3$; H_s/δ: Δ, 0.036; □, 0.072; ○, 0.14; ▽, 0.22; ●, 0.29; ■, 0.43.–, Pasquill–Gifford curves for stability classes C & D with $H_s/\delta = 0.075$, assuming geometric scale factor of 770:1.

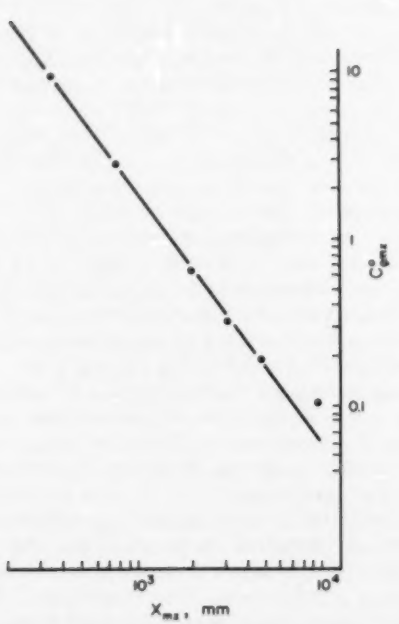

Fig. 5. Maximum surface concentration versus distance to maximum surface concentration in flat terrain.

3. RESULTS

3.1. *The flow field*

The hills will henceforth be designated by *C2S*, *C2*, *C4*, *C6* and *CX*, where the suffix *S* refers to a smooth surface hill (identical to that used by Snyder and Britter, 1979a,b, see Fig. 1). Mean velocity and turbulence measurements were made along vertical lines on $y = 0$ for $x > 0$, where x is measured from the hill centerline; spanwise traverses at fixed x and z were also made. The general aim was to deduce the shape of the three-dimensional "surface" on which the longitudinal mean velocity was zero. In all, more than 50 profiles each of the mean, variance, skewness and kurtosis were measured. Figures 8 and 9 present some typical results. Vertical profiles of mean velocity behind *C2* are shown in Fig. 8(a); corresponding longitudinal turbulent energy measurements are shown in Fig. 8(b). Figures 9(a) and 9(b) show spanwise profiles behind *C4*. Turbulent energy increases to values far in excess of those that occur in the undisturbed boundary layer and reaches peaks around the regions of maximum shear in the velocity profiles. (Of course, local turbulent intensities $\overline{u^2}/U^2$ become infinite where $U = 0$!) In the spanwise profiles this leads to a characteristic "double-humped" shape in the turbulent energy (Fig. 9b) and it is clear that the turbulent energies are relatively low deep within the cavity region, compared with values

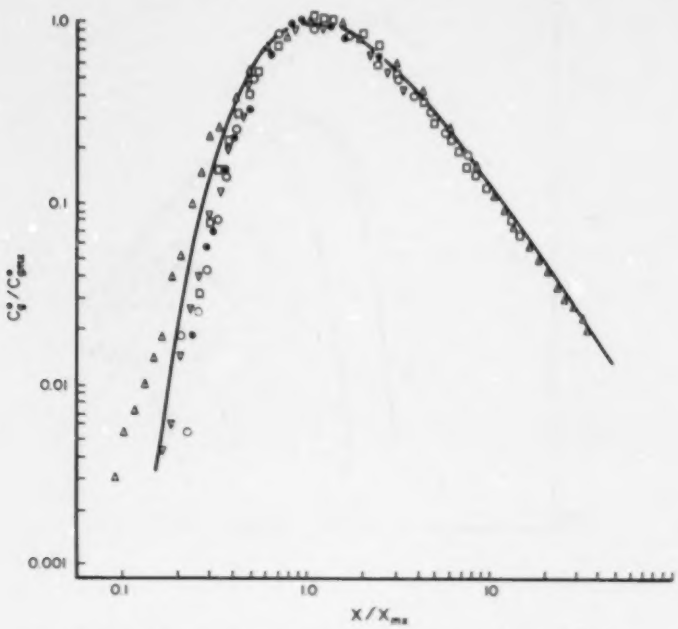

Fig. 6. Similarity of surface concentration profiles in flat terrain (legend as in Fig. 5; ——, analytic solution).

within the shear layers bounding the cavity. Figure 10 shows the locus of zero longitudinal velocity on the centerline ($y = 0$) for each hill, deduced from profiles like those in Fig. 8(a), and Fig. 11 shows similar loci in horizontal planes (at $z/h = 0.34$ and 0.8). These enable one to visualize the "surface contour of zero U-velocity" and its intersection with the ground; the latter is included in Fig. 11. Since, apart from the CX case, these are fully three-dimensional flows, it must be emphasized that this intersection is not, in general, coincident with lines of separation or reattachment and must, in fact, lie inside the latter. Only on the $y = 0$ axis of symmetry (at $x = x_R$) and, perhaps, along the (sharp) crest of the hill are the two coincident. These data, therefore, provide an accurate measure of the distance to the mean reattachment point (only on $y = 0$) and the size and shape of the volume within which the U-component of velocity is negative. In that respect they are useful measurements, but they do not allow any quantitative deductions about locations of mean streamlines, so that great care in interpreting the visual pictures provided by Fig. 11 is required.

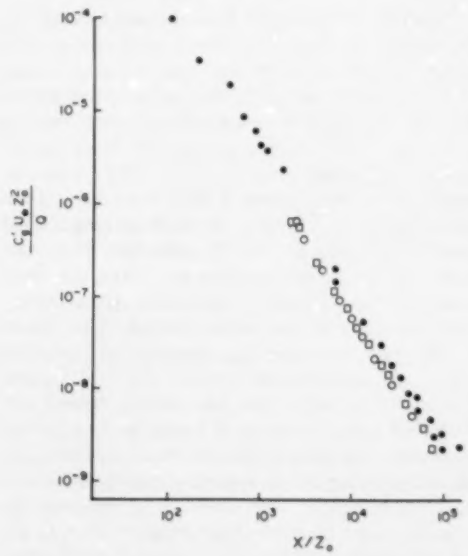

Fig. 7. Comparison of surface concentration profiles from ground level sources: ●, Robins and Fackrell, 1979; ○, Arya *et al*, 1981; □, Snyder and Britter, 1979a.

Some features are worthy of particular comment. First, it is quite clear that the reversed flow region behind the smooth cone ($C2S$) is much smaller than that behind the rough cone. Intimation of a substantial difference was provided by the earlier study of Snyder and Britter (1979), who found significant differences in surface concentrations on the lee slopes when the sources were upstream of the cones; it was this result that prompted the present direct comparison. Wilson (1980) notes that, for a smooth hill in rough terrain, the flow acceleration after the rough-to-smooth transition helps to prevent separation. The present results are in line with that suggestion, which implies an exactly opposite trend to the classic case of surface-roughened

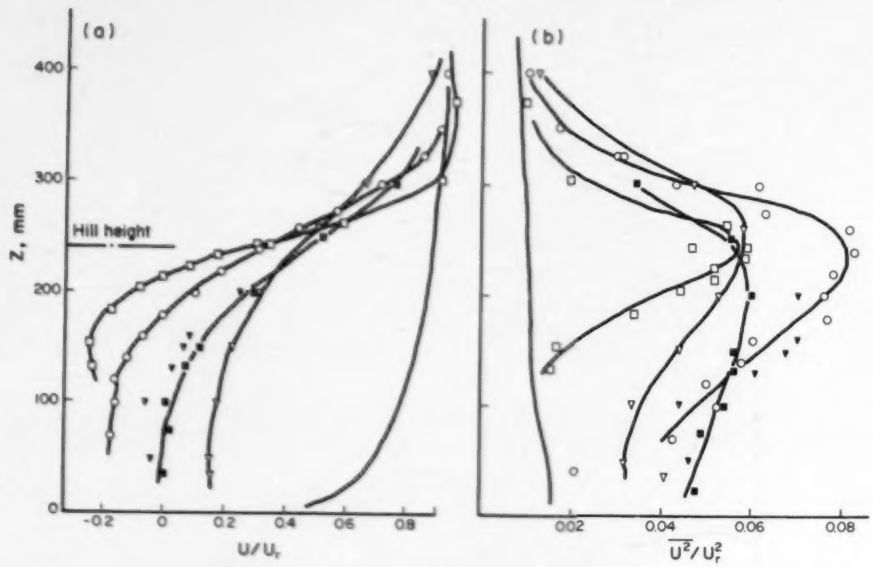

Fig. 8. Vertical profiles of (a) mean velocity and (b) longitudinal turbulent energy along center-line downwind of cone (hill *C2*): x/k: □, 0.94; ○, 1.8; ▲, 2.2; ■, 2.35; Δ, 2.82; ———, no hill.

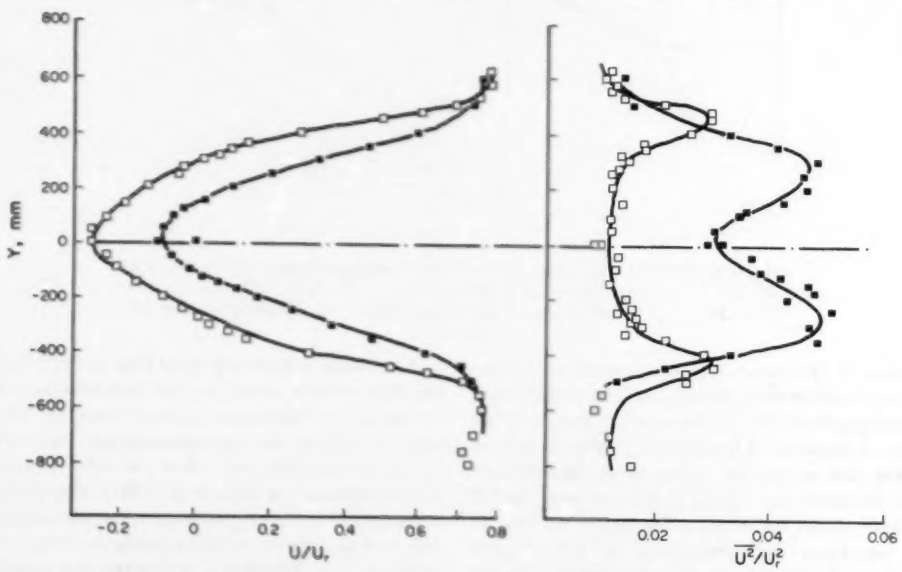

Fig. 9. Lateral profiles of (a) mean velocity and (b) longitudinal energy downwind of hill *C4*: ■, $x/h = 3.3$, $z/h = 0.33$; □, $x/h = 1.6$, $z/h = 0.33$.

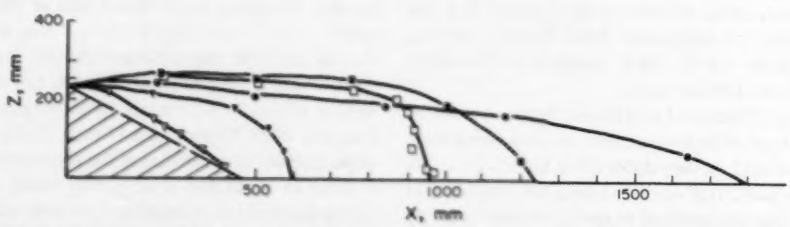

Fig. 10. Loci of zerolongitudinal-mean velocity on the centerline ($y = 0$) of the various hills: ●, *CX*, ■, *C6*, □, *C4*; ▲, *C2*; Δ, *C2S*.

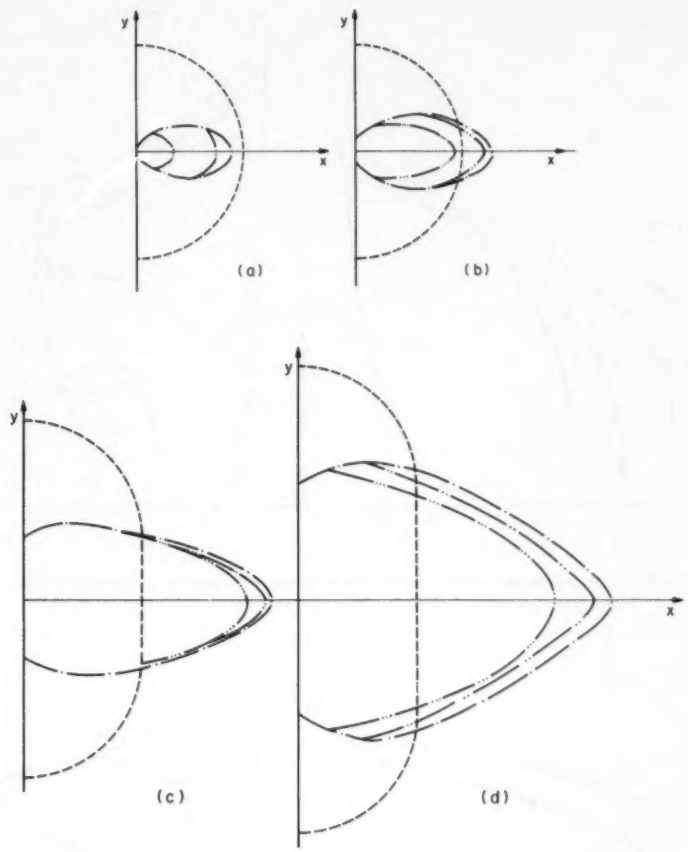

Fig. 11. Loci of zerolongitudinal–mean velocity in horizontal planes downwind of (a) *C2S*, (b) *C2*, (c) *C4* and (d) *C6*: ·——·, $z'/h = 0$; ——··——, $z/h = 0.8$; ——···——, $z/h = 0.34$; – – – –, intersection of hill surface with $z = 0$ (z' is height above hill surface).

cylinders or spheres in free flow, where the added roughness acts to delay separation. This implies that, for topographical site studies in wind tunnels where there is a dominant hill sufficiently steep to lead to possible flow separation, it may be as important to model the roughness length (z_0) appropriate to the hill as it is to model the surrounding terrain z_0. Exactly what constitutes "sufficiently steep" will depend upon the nature of the roughness transition between the hill and the surrounding surface, and while there are some tentative guidelines available in the literature (e.g. Bouwmeester, 1978; Wilson, 1980), it seems that the whole subject of separation from (usually curved) rough surfaces within thick rough-wall boundary layers requires detailed study.

Although diffusion of an effluent from a source of height $h/2$ located at, for example, the downwind base of the hill would be very different in the *C2* and *C2S* cases, we concentrated on cases where the roughness of the hill surface was identical to that of the surrounding terrain. Accordingly, no concentration measurements were made for the smooth cone (*C2S*) case.

The second notable feature of Figs 10 and 11 is that the downstream extent of the recirculating region increases with hill aspect ratio as expected, but the value of x_R/h in the "two-dimensional" limit (about 7.7) is substantially lower than the value (about 13) found indirectly by Arya *et al.* (1981). This is almost certainly due to the very different hill slopes used in the two studies. Arya *et al.* used a triangular ridge whose slope was four times that of the present case, so that the flow angle at separation was more nearly vertical. Indeed, these authors pointed out that their result was not too dissimilar from that found in the case of a simple fence (Good and Joubert, 1968), although in view of available measurements behind fences in very thick boundary layers (similar to the $\delta/h \simeq 8$ used by Arya *et al.*), $x_R/h = 13$ seems rather large (Castro and Fackrell, 1978; Ogawa and Diosey, 1980). For a hill slope midway between that of the present case and that of Arya *et al.*, Huber *et al.* (1976) found $x_R/h \simeq 9.6$, fitting the trend of increasing x_R/h with hill slope. δ/h was 3.4, 8 and 2 in these three cases, respectively, so in general it seems that x_R/h depends much more strongly

on hill slope than on the exact nature of the upstream boundary layer. These remarks strictly apply only to two-dimensional, straight-sided (and therefore sharp-crested) hills of any roughness; as indicated earlier, the behavior for hills with curved surfaces of whatever roughness is much less clear.

Finally, note that the changes in height of the centerline contour of zero velocity (Fig. 10) are not monotonic with aspect ratio. Snyder and Britter (1979) noted similar behavior in the results of their crossed-wire measurements at the crests of the hills ($x = 0$). The increase in mean velocity near the surface, for example, was lower for $C6$ than for CX, and in both cases it was lower than for $C2$. Similarly, they found a significant negative shear stress above the crests, which was greater (in magnitude) for $C4$ and $C6$ than for $C2$ and CX. The reasons for these non-monotonic trends are not obvious. It is possible that the relatively strong axial vorticity present in the wake of $C2$ (implied by the later concentration measurements, see Section 3.2.1) had a significant effect on the flow over the hill. Indeed, some of this vorticity has its origin in the horseshoe vortex, which may have more influence on the flow up the windward centerline of the cone than it would for higher aspect ratio hills.

3.2. *Concentration measurements*

Since it seemed unlikely that the flows behind hills $C4$ and $C6$ would be very different in character, the second and major stage of the work, investigation of diffusion behind each hill, was restricted to a study of hills $C2$, $C6$ and CX. The basic results of the centerline GLC measurements, from which many later deductions are made, are presented in Figs 12–14. Each plot shows the axial variation of normalized GLC for a range of source heights for a given axial source location behind a given hill, and includes the locations of both the reattachment point x_R and the source x_s.

All the data, in complete tabulated form, are available from the authors. There are various ways of replotting the data to emphasize particular features of the results and in the following sections we endeavor to point out what seem, from a fundamental point of view, the most significant and, from a practical point of view, the most useful results.

3.2.1. *Sources downstream of the cavity* ($x_s/x_R > 1$). Comparison between the results presented in Figs 12–14 and the "no-hill" baseline data (Fig. 4) shows that, for sources located beyond the cavity (at $x_s/x_R = 1.5$), the maximum GLC occurs earlier than it would in the absence of the hill and is larger by a factor which varies from about 1.5 at the lowest source height ($H_s/h = 0.25$) to about 3 at the highest ($H_s/h = 1.5$). Figure 15, in which data for all three hills are compared directly with baseline data for these extreme cases, demonstrates this clearly. Although upstream of the location of maximum GLC in the absence of the hill (x°_{max}), GLC's are always substantially higher than they would be in the absence of the hill, farther downstream they are significantly reduced, at least for low source heights (Fig. 15a). This was evident in the results of Wilson (1980) and Arya *et al.* (1981) also. It is clear too that the trends are not monotonic with aspect ratio, as

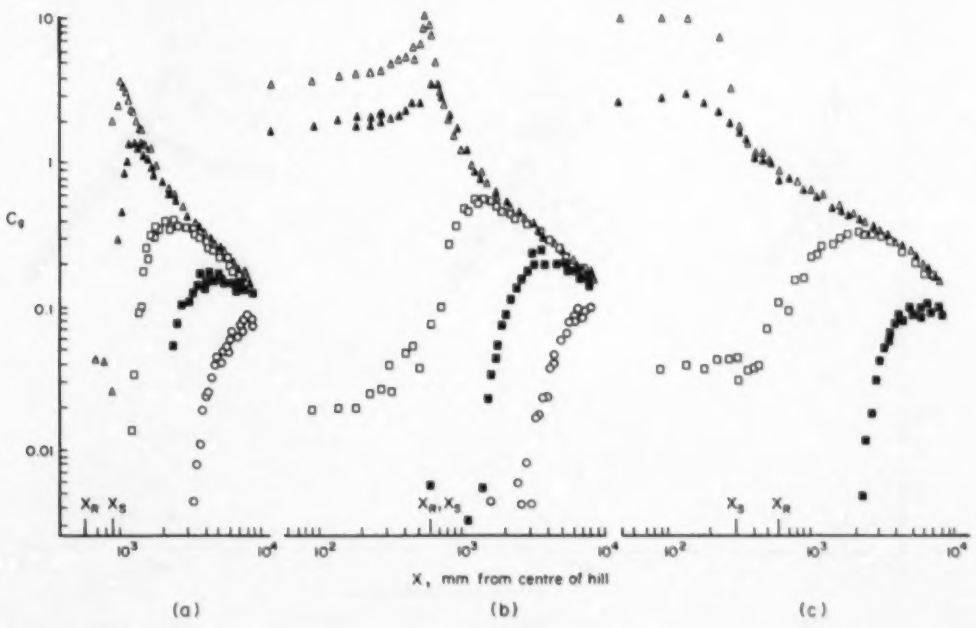

Fig. 12. Surface concentration profiles, hill $C2$: H_s/h Δ, 0.25; ▲, 0.50; □, 1.0; ■, 1.5; ○, 2.0 x_s/x_R = (a), 1.5; (b), 1.0; (c), 0.5.

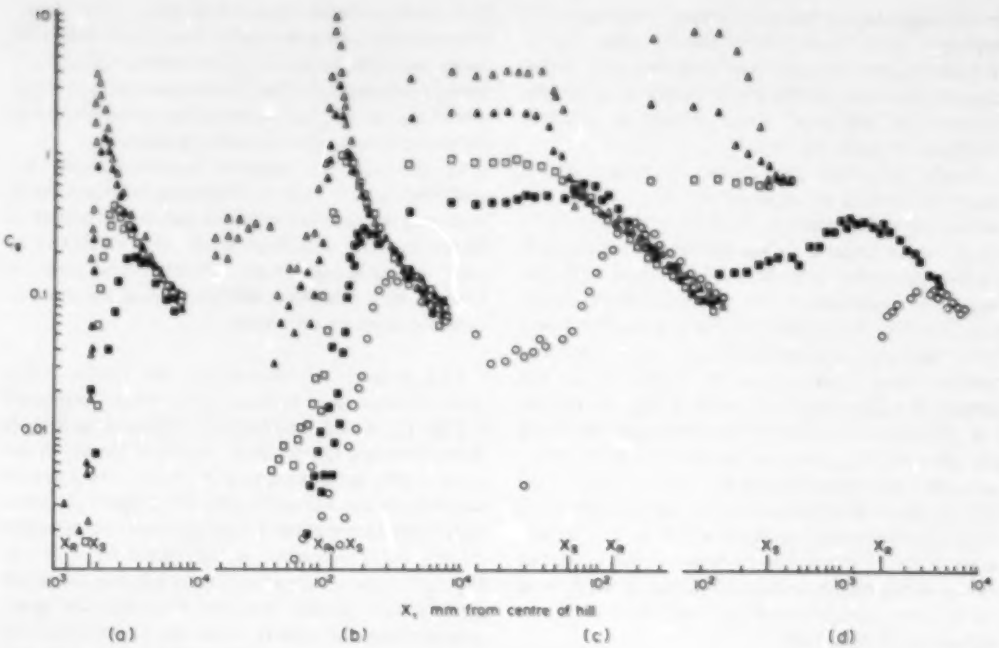

Fig. 13. Surface concentration profiles, hill *C6* (legend same as Fig. 12). x_s/x_R = (a), 1.5; (b), 1.0; (c), 0.5; (d), 0.25.

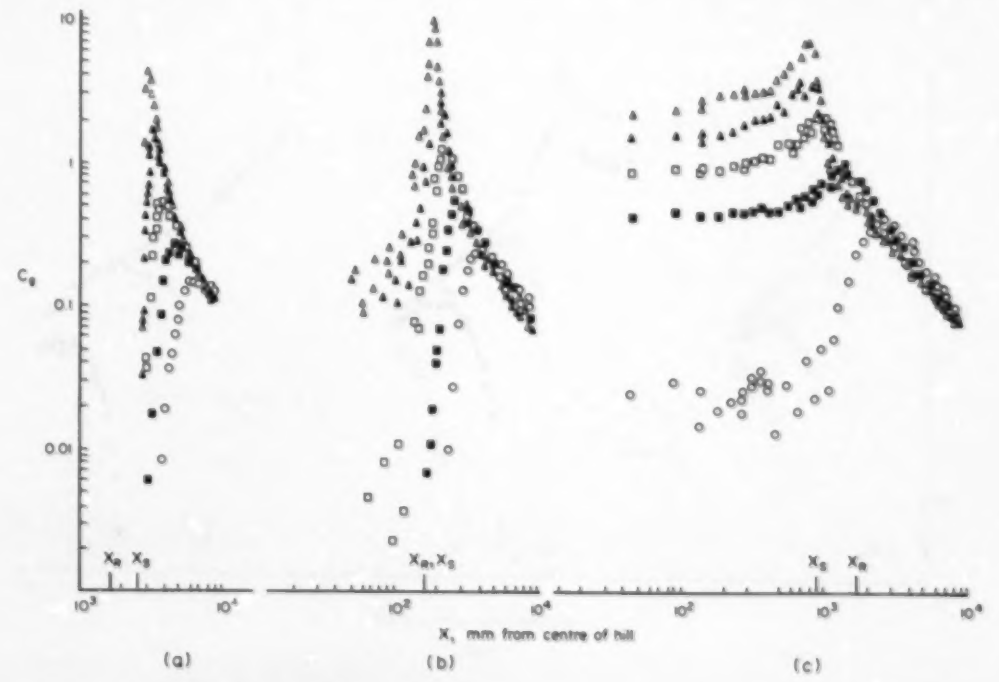

Fig. 14. Surface concentration profiles, hill *CX* (legend same as Fig. 12). x_s/x_R = (a), 1.5; (b), 1.0; (c), 0.5.

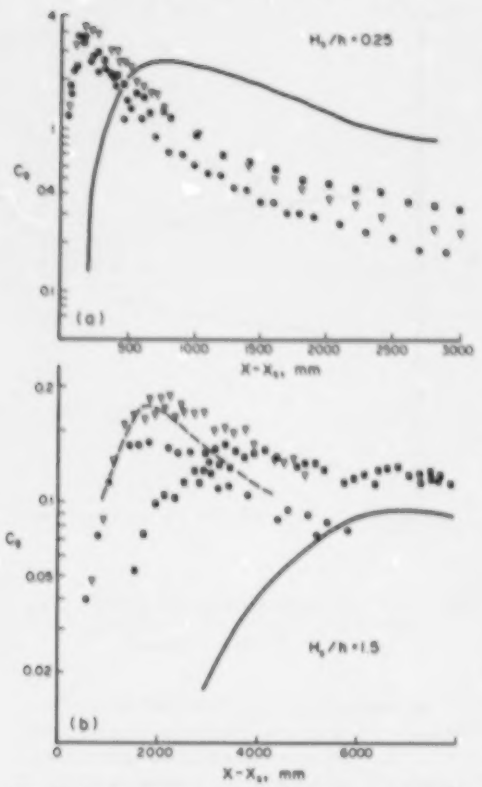

Fig. 15. Surface concentration profiles for sources located beyond the reattachment point, $x_s = 1.5x_R$: ■, *C*2: ●, *C*6; ▽, *CX* ——, no hill; – – –, Arya *et al.*, 1981. (a) $H_s/h = 0.25$; (b) $H_s/h = 1.5$.

found previously in the flow field measurements. For example, Fig. 15(b) shows that for the tallest stack the peak GLC occurs earliest for *C*6 and latest for *C*2. Similarly, Fig. 15(a) indicates that GLC's far downstream are highest for *C*2 and lowest for *C*6, but since the peak values, and their locations, are slightly different in each case, the best way of comparing decay rates of the GLC is to plot the results in similarity form, as was done for the baseline data in Section 2.2 (Fig. 6). This is done in Fig. 16 for a typical case ($H_s/h = 0.5$); there are some significant features to be noted.

First, the GLC decay beyond the peak value is very similar to that in the absence of a hill, except in case *C*2, for which it is much slower. We are not aware of any previous measurements (laboratory or field) that demonstrate this effect of hill aspect ratio. However, there have been a number of similar sets of measurements behind building-shaped bodies which have shown that for certain body shapes the axial vorticity shed into the wake (and/or arising from the horseshoe vortex which "wraps" around the body) can remain an important influence to considerable distances downstream (Lemberg, 1973; Peterka and Cermak, 1975; Robins and Castro, 1977). Recent measurements (Robins, private communication) have shown that, in the case of a square-plan body with a height only one-third of the side dimension, the GLC decay was much slower when the body was oriented at 45° to the flow direction than it was for the 0° orientation. This was almost certainly a result of much stronger axial vorticity in the wake in the 45° case and it seems likely that the results of Fig. 16 are an indirect indication of persistent longitudinal vorticity of the kind often observed in building studies. In this respect most of the

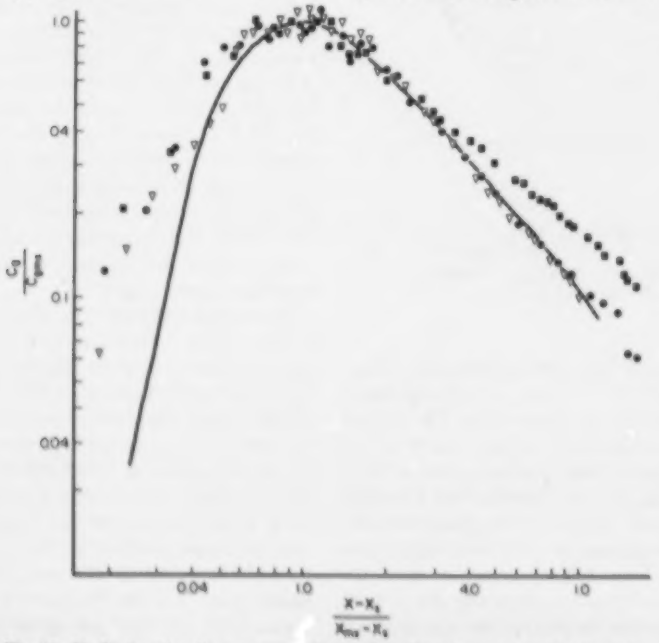

Fig. 16. Similarity of surface concentration profiles for $x_s/x_R = 1.5$ and $H_s/h = 0.5$ (legend same as Fig. 15).

downwash behind the cone may be generated by a totally different process from that leading to downwash behind two-dimensional hills. This does not imply that "near-field" downwash is stronger in that case, merely that it is more persistent. Indeed, vertical concentration profiles demonstrate just the opposite. Figure 17 shows the vertical variation of concentration at two fixed distances downstream of the source for $H_s/h = 1.0$ and hills $C2$ and CX, compared with baseline data. For both hills the plume is downwashed quite rapidly, but the effect is clearly greater for CX, where downwash is caused by only one mechanism, i.e. the descending streamlines downwind of the reattachment point. For $C2$ this downwash mechanism plus that caused by axial vorticity is clearly weaker initially, but apparently becomes relatively stronger with distance downstream.

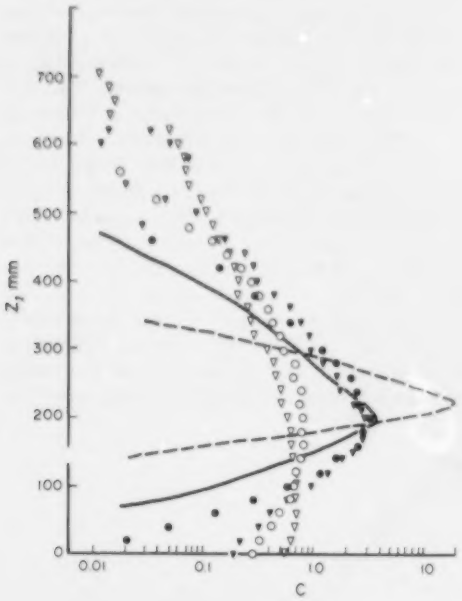

Fig. 17. Vertical concentration profiles; $x_s/x_R = 1.5$, $H_s/h = 1.0$. Hill: ○, $C2$; ▽, CX. Closed Symbols, $x - x_s = 330$ mm (no hill, – – –); Open Symbols, $x - x_s = 847$ mm, (no hill, ——).

It is interesting that peak concentrations are almost identical for hills $C2$ and CX (Fig. 17) although much lower than in the absence of the hills. The vertical plume spreading rate is, initially at least, higher for CX than for $C2$ and lateral measurements, some of which are presented in Fig. 18, show a similar behavior of the lateral spreading rate. Because of the enhanced turbulence, these spreading rates are in all cases higher than in the absence of the hill, as expected. Now the difference between GLC decay rates with and without hills must depend upon the ratio of the rates at which the vertical and lateral turbulence intensities recover to

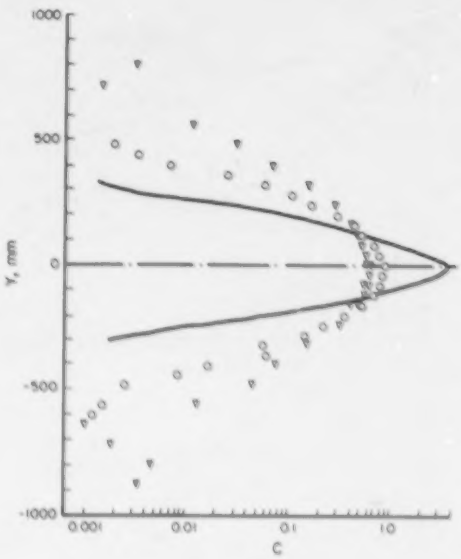

Fig. 18. Elevated lateral concentration profiles; $x_s/x_R = 1.5$, $H_s/h = 1.0$, $x - x_s = 847$ mm. $z = 180$ mm; ○, $C2$; Δ, CX; —, no hill ($z = 210$ mm).

their upstream values, since these will determine the vertical and lateral plume spreading rates. Since, for $C6$ and CX, the GLC decays at about the same rate as in the absence of the hill (Fig. 16), it seems likely that the vertical and lateral intensities recover at roughly similar rates. By contrast, the slower GLC decay behind $C2$ implies a relatively slow recovery of the lateral plume spreading rate—a probable result of persistent swirl. More detailed measurements would be required to quantify this behavior and, in particular, it would be useful to study the variation of lateral spread (σ_y) with height. Some limited measurements for hill CX showed that σ_y was not noticeably dependent on height for a source at $H_s/h = 1.0$ (and $x_s/x_R = 1.5$), as is often assumed in analytic theories of diffusion over flat terrain, but it seems probable that for flows more dominated by persistent axial vorticity—like the $C2$ case—σ_y will be rather more dependent upon height.

The second major point to note about Figs 15 and 16 is that, within a factor of about 2, the variation of surface concentration is independent of hill aspect ratio if the source is located at the same x_s/x_R and H_s/h in each case. This lends support to the hypothesis discussed in Section 1, that we might find similarity in the diffusion patterns behind all hills when scaling with x_R. It suggests that surface concentrations for a given stack height and downwind location could be estimated independently of hill shape, provided only that x_R could be estimated. It is also possible that the hill height (relative to the boundary-layer height) is, like aspect ratio, relatively unimportant: Figure 15(b) includes results obtained by Arya *et al.* (1981) for a much

steeper two-dimensional hill and a source at $x/h = 15$ and $H_s/h = 1.5$; x_s/x_R was not too different from the value of 1.5 appropriate to the other cases in the figure. The results lie within the range of the present measurements, even though h/δ was only 40% of that in the present case. Further work would be necessary to substantiate that hill height is not important, but this conclusion is, in any case, unlikely to be valid for hills which have sufficiently low slopes to prevent separation. (h/δ must become an important parameter far downstream.) Even if one could choose an appropriate "x_s/x_R", for such hills, the inevitably lower turbulence levels would presumably lead to a GLC profile somewhere between the hill and no-hill cases shown in Fig. 15.

The practically useful results concerning the effect of hill aspect ratio and source position on the amplification A of the peak GLC will be presented in Section 3.3.

3.2.2. *Sources near or within the cavity* ($x_s/x_R \leqslant 1$). When effluent is emitted close to the outer boundary of the recirculating region, the peak GLC should be near $x = x_R$, because the streamline through the source will reattach to the surface there. Figure 19 shows the data for all three hills with $x_s = x_R$, $H_s/h = 0.25$, and, clearly this case, at least, confirms the expectation. Furthermore, since mean velocities are very low in that region, turbulent diffusion dominates the near field dispersion, and the GLC distributions are approximately symmetric for values down to about an order of magnitude less than the maximum. Again it seems that, at least for $x > x_s$, GLC values are, within a factor of two, independent of hill aspect ratio. The peak value is about four times that in the absence of the hill, but beyond about $x_s + 6H_s$, GLC's are significantly lower than in the no-hill case.

In Figure 20, the results for $H_s/h = 1.5$ and 2.0, $x_s/x_R = 0.5$, are compared for hills *C*6 and *CX*. The reattachment locations x_R are included in the figure and, while accurate interpolation is difficult, the results suggest that source heights around 1.7 to 1.8h would lead to peak GLC's occurring at $x = x_R$. This height is evidently quite close to the height of the mean reattaching streamline and reference to Fig. 10 indicates that this streamline is relatively closer to the line of zero-longitudinal velocity in the *C*6 case than it is for *CX*. This is plausible, since the three-dimensional nature of the *C*6 flow allows some recirculating fluid to be supplied (and lost) through the "sides" of the cavity. For the extreme case of the cone (*C*2), the peak GLC is well downstream of reattachment even for $H_s = h$ (see Fig. 12c), so that here the reattaching streamline must be even closer to the $U = 0$ locus (at least at $x_s/x_R = 0.5$) than it is for *C*6, confirming the trend suggested by the *C*6 and *CX* results.

One result of this variation in height of the cavity zone with aspect ratio is that GLC's do not collapse when x_s/x_R is constant, for a particular H_s. Although the *C*6 and *CX* results shown in Fig. 20 are, again, within a factor of two of one another, the *C*2 results (not shown) are quite different. If, however, the sources were located so that H_s/H_{rs} was constant, where H_{rs} is the height of the reattaching streamline, then possibly the GLC's would again collapse and be independent of hill aspect ratio. Our measurements were not sufficiently extensive to check that hypothesis.

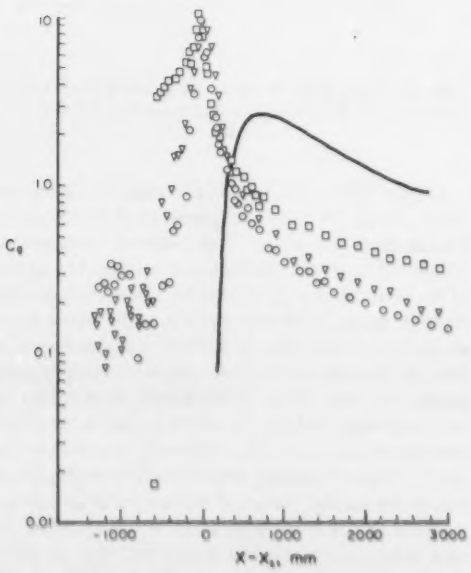

Fig. 19. Surface concentration profiles with $x_s/x_R = 1.0$ and $H_s/h = 0.25$; —, no hill; □, *C*2; ○, *C*6; ▽, *CX*.

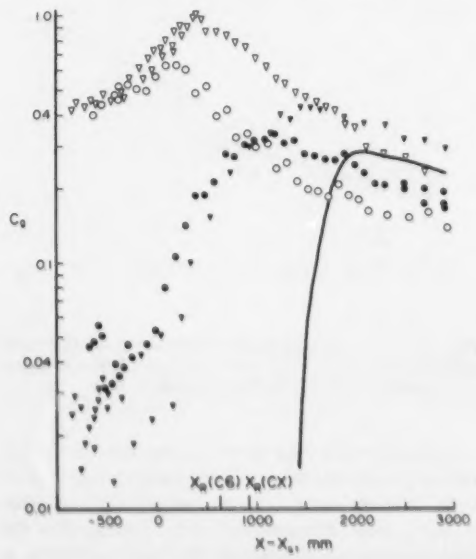

Fig. 20. Surface concentration profiles with $x_s/x_R = 0.5$ and tall sources. $H_s/h = 1.5$; no hill, —; ○, *C*6; ▽, *CX*. Solid symbols, $H_s/h = 2.0$.

For sources well within the recirculating region (i.e. below the $U = 0$ locus), the peak GLC always occurs upstream of x_s, because mean advection velocities are actually upwind (with respect to the free-stream velocity). It is often suggested in the literature that concentrations within the cavity will be roughly constant (e.g. Puttock and Hunt, 1979), but the present results (Fig. 21) demonstrate large variations of GLC's within the cavity for sources both deep inside it ($H_s/h = 0.25$) and just outside it ($H_s = 2.0$) at $x_s/x_R = 0.5$. In both cases there are order of magnitude variations in the surface concentrations; for $H_s/h = 2.0$, the concentration near x_R is about ten times that near the hill peak (i.e. near separation), while for $H_s/h = 0.25$, the reverse is true. In the latter case there would also be large variations in the vertical concentration profiles, particularly near the source itself, but for the case of sources above the cavity region, measurements showed that the concentration near the top of the cavity was lower than the surface value (at the same x) by only a factor of about two. Arya *et al.* (1981) have also reported wide variations of concentration within separated regions; thus, theoretical models of diffusion processes which assume a constant cavity concentration may not be realistic.

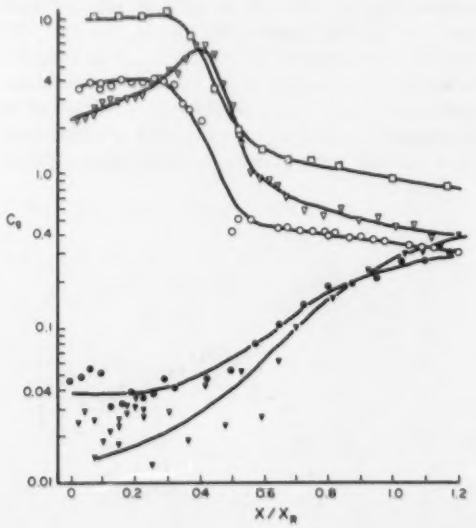

Fig. 21. Surface concentrations within cavity for short and tall sources at $x_s/x_R = 0.5$. Hill: □, *C2*; ○, *C6*; ▽, *CX*; Open symbols, $H_s/h = 0.25$; Closed symbols, $H_s/h = 2.0$.

Figure 21 (and Figs 12–14) shows that, on the hill side of sources placed within the cavity, a region does exist where the concentration is roughly constant. This occurs a little "downstream" of the source, after the initial rise in the direction of the mean advection; it suggests that a well mixed region exists near the hill, before the mean streamlines reverse direction. With further diffusion out of the recirculation zone, a significant drop in concentrations occurs beyond the source.

A few lateral profiles of cavity concentration were measured and Fig. 22 presents some of the more interesting results, for a case where $H_s/h = 0.25$, $x_s/x_R = 0.5$ (hill *CX*). Lateral profiles of surface concentration both beneath the source and nearer the hill (i.e. farther downstream in terms of the local flow direction) are shown. They both have shapes characteristic of very narrow plumes (arising from immediate advective and diffusive effects) superimposed on much wider and weaker background plumes that arise no doubt from the recirculation, with subsequent spreading and diluting of this initial narrow plume. The profile at $x = x_R$, also included in the figure, does not show this effect.

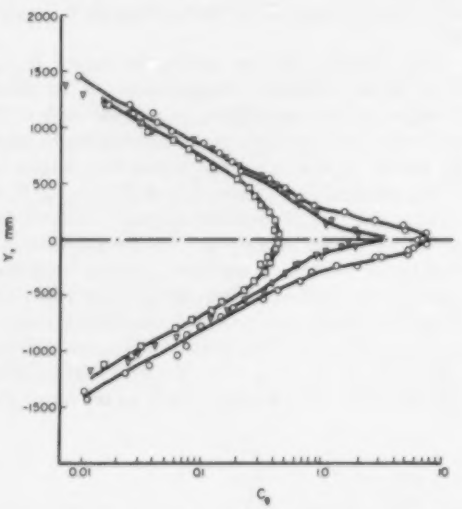

Fig. 22. Lateral surface concentration profiles for hill *CX* with $x_s/x_R = 0.5$ and $H_s/h = 0.25$: x/x_R: ○, 0.4; ▽, 0.5; □, 1.0.

In cases where the source was outside the cavity but close enough for significant amounts of source gas to be entrained into it, the results showed more scatter within the cavity than farther downstream. The length of the cavity zone undoubtedly fluctuates considerably (indeed, the re-attachment point is really only a mean statistical concept). Recent work has suggested that, at least for two-dimensional reattachment, the time scale associated with these cavity-length fluctuations is relatively large (Eaton *et al.*, 1979), so that in the above case source gas is only intermittently returned to the cavity; longer averaging times would be necessary to reduce the scatter. Ratios of the temporal maximum-to-mean values of concentration would therefore be very large throughout the cavity, and Fig. 23 demonstrates that that is in fact the case. For sources well within the cavity, C_{ms}/C_{mean} should also be relatively large near $x = x_s$, because of the reversing nature of the

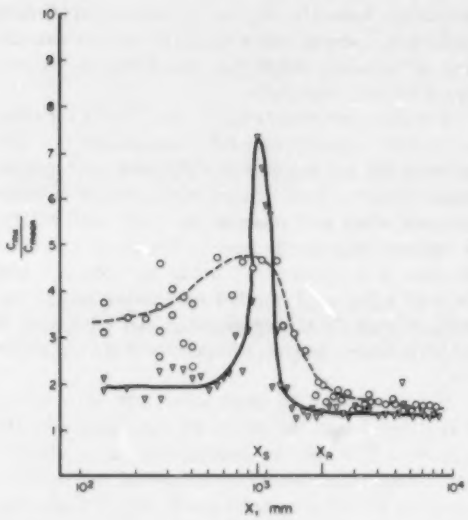

Fig. 23. Maximum one-second concentration values from two-minute record lengths as functions of position in cavity downwind of CX; H_s/h: ∇, 0.25; ○, 2.0.

advection there; a further set of data included in Fig. 23 confirms that.

Finally, for a given source height, the maximum GLC's do not necessarily occur for sources within the cavity. Comparison of Figs 13(a), (b) and (c) shows that the peak concentration obtained with a source inside the cavity is actually exceeded for sources (of the same height) beyond the cavity—up to $x_s = 1.5\,x_R$—at least for low source heights. Detailed discussion of amplification ratios is given in the following section.

4. FURTHER DEDUCED RESULTS

From a practical point of view, it is useful to define "worst cases"—for example, under what conditions is the GLC at its maximum in the presence of an upstream hill? A, the ratio of the peak GLC in the presence of the hill C_{gmx} to that in its absence C^o_{gmx} for the same source height, has been calculated from the data (Fig. 24). A two-dimensional hill leads to the largest values of A and, in general, the source height which gives the maximum A tends to increase as the source is moved nearer to the hill (Fig. 24a). The maximum A occurs for source heights comparable to the hill height in the CX case, and is reduced as the hill aspect ratio decreases.

For $C2$, in contrast to the CX case, the largest A's for high sources occur when the source is located near the end of the cavity zone rather than well within it. This is emphasized in Fig. 24(b), where A is plotted as a function of source location, for both low and high sources. For low sources ($H_s/h = 0.50$), there is a reasonable collapse of the data for all three hills, particularly for sources beyond the end of the cavity, again substantiating our hypothesis in Section 1 that scaling source locations on x_R should lead to approximate similarity in the concentration field downstream of reattachment. For high sources ($H_s/h = 1.5$) there is no collapse: for $x_s < x_R$, because of the differing vertical extent of the wake in the separated region (see Section 3.2) and, for $x_s > x_R$, because the peak GLC values occur much farther downstream, so are more influenced by the different downwash behavior behind each hill (see Section 3.2.1). Even for high sources, however, the A values do not differ by more than a factor of about two for sources beyond the cavity, as implied by the results discussed in Section 3.2.1.

The maximum A's obtained for $H_s/h = 0.5$ are greater for $C2$ than for $C6$ (although the difference is small), whereas for $H_s/h = 1.5$, the reverse is true. The conditions giving the largest A values are not, in general, those that lead to the greatest absolute GLC values: these invariably occur, of course, for low sources within, or near, the cavity region.

Frequently, the effects of hills (or buildings) on the peak GLC's are assessed by determining the "effective" source height, H_e—the height of the source in the

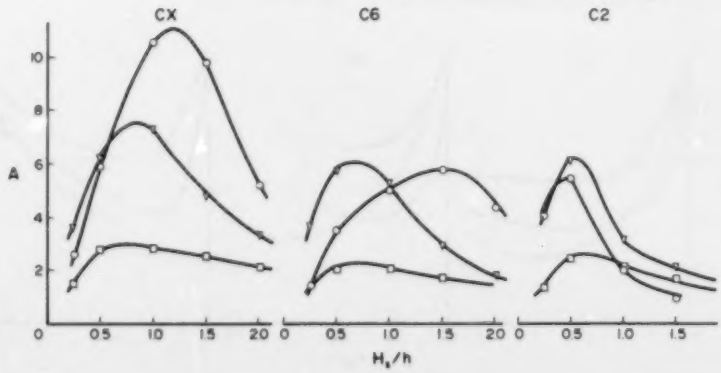

Fig. 24(a).

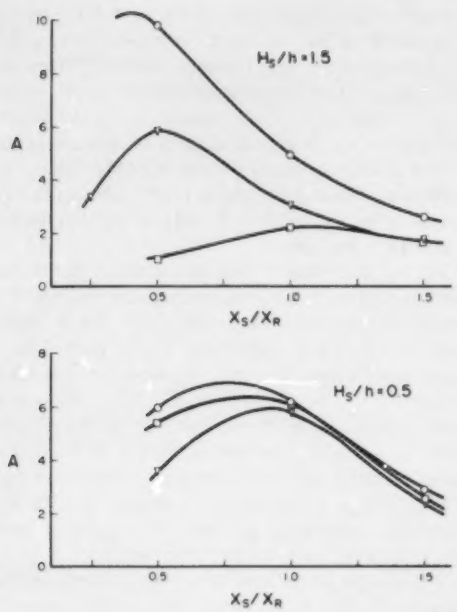

Fig. 24. Variation of amplification factor. (a) with stack height. x_s/x_R; 0, 0.5, ∇, 1.0; □, 1.5. (b) with source position downwind. □, *C2*; ∇, *C6*; 0, *CX*.

absence of the hill that would give the same peak GLC as that obtained in its presence. Figure 25 shows the variation of H_e with H_s for each of the present cases. (Note that since, for *C2*, $x_s/x_R = 0.5$ corresponds to a location actually over the hill surface, it is not possible to make a proper comparison of the data for that case, except perhaps for the sources that are well above the cavity, so that peak GLC's are not affected by the local hill height.) The lowest H_e must occur at the same H_s which gives the maximum A (cf. Fig. 24a). The most significant feature of Fig. 25 is that H_e depends more on source location x_s than on the hill aspect ratio, particularly for the lower source heights ($H_s/h \lesssim 1.0$), as might have been expected from the previous results. In addition, for $H_s/h \gtrsim 1.0$, H_e/H_s increases as x_s/x_R increases, whereas for $H_s/h \lesssim 1.0$, the greatest effective reduction in source height occurs for sources near the end of the cavity rather than well within it—again a result implied previously.

It is clear from Figs 24 and 25 that, for *C2*, the effect of the hill is minimal only for source heights in excess of twice the hill height. For wider hills, even greater source heights would be necessary to ensure a similar minimal effect and since, in the field, stack heights would not often greatly exceed hill heights for obvious reasons, it is evident that, unless the source is well beyond $x_s/x_R = 1.5$, the hill will always lead to significant peak GLC amplifications and reductions in effective source heights, irrespective of the hill aspect ratio.

Finally, it must be emphasized that, as a referee has pointed out, the effects of stratification in the upstream flow may be dominant as far as effective stack-height determination is concerned, so that application of the present results should only be made after suitable analysis of the particular location's meteorology.

5. FINAL DISCUSSION AND CONCLUSIONS

Some of our results can be usefully applied in full-scale situations, but there are clearly some aspects of the general problem that have not been considered. Perhaps most important are the effects of stratification in the upwind flow and the effects of changes in wind direction. It is not appropriate here to discuss effects of non-neutral stratification, but some comments on the effects of wind direction are in order.

Only mean flows normal to the longer axis of the hill have been studied. For axisymmetric hills (like *C2*) a change in mean wind direction is equivalent to moving the source off the centerline ($y = 0$), which will invariably lead to a reduction in the effect of the hill. Because of the well-known variability in mean wind direction in the atmosphere, full-scale amplifications will almost always be lower than those measured in wind tunnel tests. Thus, our results for *C2* are probably pessimistic, and further work is necessary to quantitate the effect.

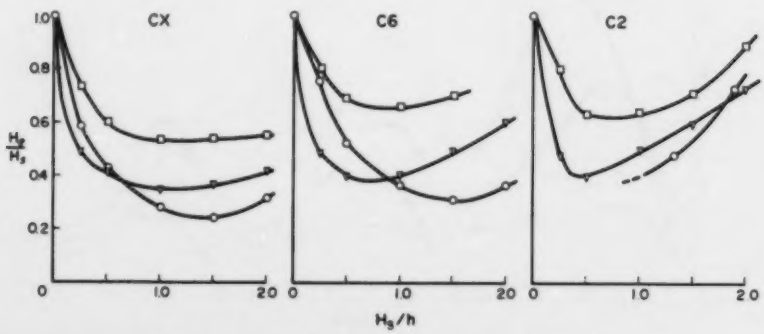

Fig. 25. Effective stack heights. Legend same as Fig. 24(a).

For higher aspect ratio hills, however, the opposite trend may occur. A shift in wind direction away from a line perpendicular to the ridge may amplify the axial vorticity, tending to counteract the other apparent effect of moving the source off the centerline. Further work is necessary to discover which effect will dominate and to estimate changes in peak GLC's.

We have investigated cases in which the hill is sufficiently steep to promote separation and to ensure a relatively large "cavity" zone. Turbulence intensities in the wake will be considerably lower in cases where no mean flow reversals occur so that, again, the present results are probably only applicable to this "worst case" situation. The results can be summarized as follows:

(1) The position of separation and the consequent size of the recirculating region can depend significantly on changes in surface roughness. For the axisymmetric hill (*C2*) it was found that a smooth hill surface led to a delay in separation and a much smaller reversed flow region. In specific site investigations, therefore, any roughness transitions that occur on hill surfaces should be modeled.

(2) Comparing our results to those of Huber *et al.* (1976), Khurshudyan *et al.* (1981) and others, it seems that hill slope upstream of the ridge is more important in determining the length of the recirculating region than the precise character of the upstream flow unless, of course, the flow is not neutral. Significant effects of stratification have been discussed elsewhere (e.g. Hunt and Snyder, 1980).

(3) Both flow field and concentration data have shown that changes in the structure of the wake and resulting concentration patterns are not necessarily monotonic with changes in hill aspect ratio. Downwash can be caused by different mechanisms and this finding may therefore be a reflection of the superposition of the various "downwash phenomena"; one process sometimes dominates the others.

(4) For axisymmetric hills, a significant mechanism producing downwash is axial vorticity in the wake. This appears to be particularly persistent, so that the decay of the centerline surface concentration downwind of its maximum value is noticeably slower than it is behind hills of higher aspect ratio. Even for a hill whose mid-height spanwise width is only about six times its height, the decay rate is not distinguishable from that behind a "two-dimensional" hill, so that end-effects rapidly become insignificant as far as that feature of the flow is concerned.

(5) For sources located beyond the recirculating region such that $x_s = cx_R$ $(c > 1)$, the centerline surface concentrations are, for practical purposes, independent of aspect ratio. There is never more than a factor of about two difference in GLC's as aspect ratio varies, and even this variability occurs only for source heights relatively close to the hill height. For $H_s \leqslant 0.75$ or $\geqslant 1.5$, the changes with aspect ratio are much lower. To engineering accuracy, therefore, recovery of the turbulence field to the undisturbed state and/or swirling motions in the wake are not so dependent on hill aspect ratio that large differences occur in, for example, peak GLC's. Figure 26, prepared from plots like Figs 24 and 25, could be used to estimate amplification factors in real situations, providing only that a reasonable estimate for x_R could be made. Provided that separation still occurs, we do not believe that changes in hill slope would affect these results significantly. Note that under no circumstances does the amplification factor exceed about seven.

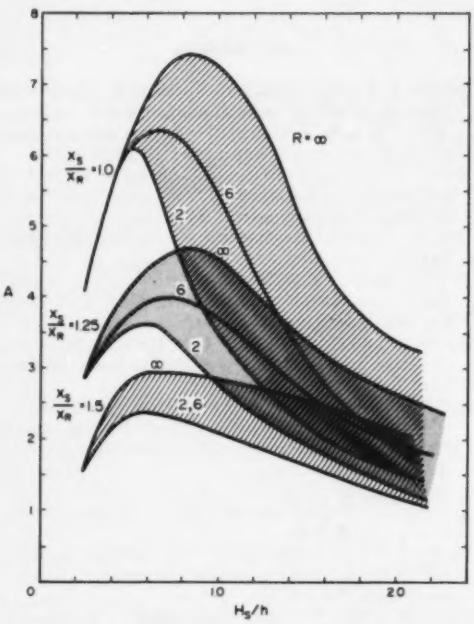

Fig. 26. Variation of amplification factor for sources downwind of reattachment point (R = aspect ratio).

(6) For sources above the cavity but close to the mean reattaching streamline, peak GLC's occur near x_R and can, for very wide hills, exceed the no-hill value by an order of magnitude. Farther downstream, however, beyond about $x_R + 6H_s$, concentrations are much lower than in the absence of the hill because lateral and vertical plume widths are increased by the high levels of turbulence in the near wake. In this case, aspect ratio effects are much more significant, probably because we used the same H_s values for each hill. The vertical extent of the recirculating region varies considerably with aspect ratio. If H_s/H_{rs} were kept constant, the results may well demonstrate a much weaker dependence on aspect ratio. That case is, however, of less practical importance than the $x_s > x_R$ situation.

(7) For sources located within the recirculating region, the surface concentration along the center-

line is far from constant: order-of-magnitude variations occur independent of hill aspect ratio.

(8) For sources within or above the recirculating region, Figs 24 and 25 can be used to estimate amplification factors and effective stack heights likely to occur in real situations.

Acknowledgements—The authors wish to thank the staff of the EPA Fluid Modeling Facility for their cooperation during the course of this study, in particular, Messrs. R. Jones and W. Pendergrass, who undertook the majority of the experimental work. IPC is grateful for support from North Carolina State University as a Visiting Assistant Professor, through EPA Grant R805595.

REFERENCES

Arya S. P. S. and Shipman M. S. (1981) An experimental investigation of flow and diffusion in the disturbed boundary layer over a ridge—I. Mean flow and turbulence structure. *Atmospheric Environment* **15**, 1173–1184.

Arya S. P. S., Shipman M. S. and Courtney L. Y. (1981) An experimental investigation of flow and diffusion in the disturbed boundary layer over a ridge—II. Diffusion from a continuous point source. *Atmospheric Environment* **15**, 1185–1194.

Bouwmeester R. J. B. (1978) Wind characteristics over ridges. Ph.D. dissertation, Department of Civil Engineering, Colorado State University, Ft. Collins, CO.

Bradbury L. J. S. and Castro I. P. (1971) A pulsed-wire technique for velocity measurements in highly turbulent flows. *J. Fluid Mech.* **49**, 657–691.

Britter R. E. and Hunt J. C. R. (1979) Velocity measurements and order of magnitude estimates of the flow between two buildings in a simulated atmospheric boundary layer. *J. ind. Aero.* **4**, 165–182.

Castro I. P. and Fackrell J. E. (1978) A note on two-dimensional fence flows with emphasis on wall constraint. *J. ind. Aero.* **3**, 1–20.

Castro I. P. and Robins A. G. (1977) The flow around a surface-mounted cube in uniform and turbulent streams. *J. Fluid Mech.* **79**, 307–335.

Coles D. (1956) The law of the wake in the turbulent boundary layer. *J. Fluid Mech.* **1**, 191.

Counihan J. (1969) An improved method of simulating an atmospheric boundary layer in a wind tunnel. *Atmospheric Environment* **3**, 197–214.

Counihan J. (1975) Adiabatic atmospheric boundary layers: A review and analysis of data from the period 1880–1972. *Atmospheric Environment* **9**, 871–905.

*Courtney L. Y. and Britter R. E. (1979) Measurements of velocity and concentration in a simulated atmospheric boundary layer. Environmental Protection Agency Report (in preparation), Research Triangle Park, NC.

Davies M. E., Quincey V. G. and Tindall S. J. (1980) The near-wake of a tall building block in uniform and turbulent flows. *Wind Engineering, Proc. 5th Int. Conf.*, Ft. Collins, CO, July 1979 (Edited by J. E Cermak) **1**, 289–298.

Eaton J. K., Johnston J. P. and Jeans A. H. (1979) Measurements in reattaching shear layers. 2nd Symp. on Turbulent Shear Flows, Imperial College, London.

Good M. C. and Joubert P. N. (1968) Form drag of two-dimensional bluff plates immersed in turbulent boundary layers. *J. Fluid Mech.* **31**, 547–582.

Halitsky J. (1968) Gas diffusion near buildings. In *Meteorology and Atomic Energy* (Edited by D. H. Slade) TID-24190, U.S. Atomic Energy Commission, 221–255.

Huber A. H., Snyder W. H., Thompson R. S. and Lawson R. E., Jr. (1976) Stack placement in the lee of a mountain ridge: A wind tunnel study. Environmental Protection Agency Report No. EPA-600/4-76-047, Research Triangle Park, NC.

Hunt J. C. R., Abell C. J., Peterka J. A. and Woo H. (1978) Kinematical studies of the flows around free or surface-mounted obstacles: Applying topology to flow visualization. *J. Fluid Mech.* **86**, 179–200.

Hunt J. C. R. and Snyder W. H. (1980) Experiments on stably and neutrally stratified flow over a model three-dimensional hill. *J. Fluid Mech.* **96**, 671–704.

*Khurshudyan L. H., Snyder W. H. and Nekrasov I. V. (1981) Flow and dispersion of pollutants over two-dimensional hills: Summary report on joint Soviet–American study. Environmental Protection Agency Report (in press), Research Triangle Park, NC.

Lemberg R. (1973) On the wakes behind bluff bodies in a turbulent boundary layer. Report No. BLWT-3-73, Boundary Layer Wind Tunnel Laboratory, University of Western Ontario, London, Ontario, Canada.

Moore D. J. (1975) A simple boundary-layer model for predicting time mean ground-level concentrations of material emitted from tall chimneys, *Proc. Inst. mech. Engrs* **189**, 33–43.

Ogawa Y. and Diosey P. G. (1980) Surface roughness and thermal stratification effects on the flow behind a two-dimensional fence, Part I: Field Study. *Atmospheric Environment* **14**, 1301–1308.

Ogawa Y. and Diosey P. G. (1980) Surface roughness and thermal stratification effects on the flow behind a two-dimensional fence, Part II: A wind tunnel study and similarity considerations. *Atmospheric Environment* **14**, 1309–20.

Pasquill F. (1974) *Atmospheric Diffusion.* (2nd Edition), Chichester, Ellis Horwood, John Wiley, New York, NY.

Peterka J. A. and Cermak J. E. (1975) Turbulence in building wakes. 4th Intl. Conf. on Wind Effects on Buildings and Structures, Sept. 8–12, London, England (also Report no. CER74-75JAP-JEC34, Colorado State University, Ft. Collins, CO).

Puttock J. S. and Hunt J. C. R. (1979) Turbulent diffusion from sources near obstacles with separated wakes—I. An eddy diffusivity model. *Atmospheric Environment* **13**, 1–13.

Robins A. G. (1978) Plume dispersion from ground-level sources in simulated atmospheric boundary layers. *Atmospheric Environment* **12**, 1033–1044.

Robins A. G. (1979) The development and structure of simulated neutrally stable atmospheric boundary layers. *J. ind. Aero.* **4**, 71–100.

Robins A. G. and Castro I. P. (1977) A wind tunnel investigation of plume dispersion in the vicinity of a surface mounted cube—I. The flow field. *Atmospheric Environment* **11**, 291–297.

Robins A. G. and Castro I. P. (1977) A wind tunnel investigation of plume dispersion in the vicinity of a surface mounted cube—II. The concentration field. *Atmospheric Environment* **11**, 299–311.

Robins A. G. and Fackrell J. E. (1979) Continuous plumes—their structure and prediction. Central Electricity Generating Board Memo. No. MM/MECH/TF148, Marchwood, England.

Scorer R. S. (1968) *Air Pollution.* Pergamon Press, New York, NY, 151p.

Snyder W. H. (1979) The EPA Meteorological Wind Tunnel: Its design, construction and operating characteristics. Environmental Protection Agency Report No. EPA-600/4-79-051, Research Triangle Park, NC.

*Snyder W. H. and Britter R. E. (1979a) Sanspray boundary layer characterization. Data Report (unpublished), Fluid Modeling Facility, Environmental Protection Agency, Research Triangle Park, NC.

*Snyder W. H. and Britter R. E. (1979b) Aspect ratio study.

* These reports, although not yet published in the open literature, are available from the second author (WHS).

Data Report (unpublished), Fluid Modeling Facility, Environmental Protection Agency, Research Triangle Park, NC.

Strom G. H. (1976) Transport and diffusion of stack effluents. In *Air Pollution*, Vol. 1, (3rd Edition) (Edited by A. C. Stern) Academic Press, New York, NY.

Turner D. B. (1970) *Workbook on Atmospheric Dispersion Estimates*. Publ. No. AP-26, Environmental Protection Agency, Research Triangle Park, NC.

Williams H. P. and Winefordner J. D. (1966) Construction and operation of a single exponential dilution flask for calibration of gas chromatographic detectors, *J. Gas Chrom.* 271–272.

Wilson D. J. (1980) Influence of a hill ridge on ground-level concentration of stack gas plumes. *Envir. Technol. Lett.* **1**, 177–184.